International Journal of Polymeric Materials and Polymeric Biomaterials

ISSN: 0091-4037 (Print) 1563-535X (Online) Journal homepage: https://www.tandfonline.com/loi/gpom20

Cation-mediated gelation of the fucose-rich polysaccharide FucoPol: preparation and characterization of hydrogel beads and their cytotoxicity assessment

Letícia Fialho, Diana Araújo, Vitor D. Alves, Catarina Roma-Rodrigues, Pedro V. Baptista, Alexandra R. Fernandes, Filomena Freitas & Maria A. M. Reis

To cite this article: Letícia Fialho, Diana Araújo, Vitor D. Alves, Catarina Roma-Rodrigues, Pedro V. Baptista, Alexandra R. Fernandes, Filomena Freitas & Maria A. M. Reis (2021) Cation-mediated gelation of the fucose-rich polysaccharide FucoPol: preparation and characterization of hydrogel beads and their cytotoxicity assessment, International Journal of Polymeric Materials and Polymeric Biomaterials, 70:2, 90-99, DOI: 10.1080/00914037.2019.1695205

To link to this article: https://doi.org/10.1080/00914037.2019.1695205

Published online: 23 Nov 2019.

Submit your article to this journal

Article views: 217

View related articles

View Crossmark data

Citing articles: 5 View citing articles

Full Terms & Conditions of access and use can be found at
https://www.tandfonline.com/action/journalInformation?journalCode=gpom20

INTERNATIONAL JOURNAL OF POLYMERIC MATERIALS AND POLYMERIC BIOMATERIALS
2021, VOL. 70, NO. 2, 90–99
https://doi.org/10.1080/00914037.2019.1695205

Taylor & Francis
Taylor & Francis Group

Check for updates

Cation-mediated gelation of the fucose-rich polysaccharide FucoPol: preparation and characterization of hydrogel beads and their cytotoxicity assessment

Letícia Fialho[a,b], Diana Araújo[a], Vitor D. Alves[c], Catarina Roma-Rodrigues[b], Pedro V. Baptista[b], Alexandra R. Fernandes[b], Filomena Freitas[a], and Maria A. M. Reis[a]

[a]UCIBIO-REQUIMTE, Chemistry Department, Faculdade de Ciências e Tecnologia, Universidade Nova de Lisboa, Caparica, Portugal; [b]UCIBIO, Departamento Ciências da Vida, Faculdade de Ciências e Tecnologia, Universidade Nova de Lisboa, Caparica, Portugal; [c]LEAF, Linking Landscape, Environment, Agriculture and Food, Instituto Superior de Agronomia, Universidade de Lisboa, Caparica, Portugal

ABSTRACT

This study describes for the first time the iron- and copper-mediated gelation of FucoPol, fucose-rich bacterial polysaccharide. The ability of FucoPol to gel in the presence of metal cations, including iron(III) and copper(II), was used for the preparation of hydrogel beads. Iron mediated the formation of stable and not cytotoxic gel beads, while copper resulted in fragile and cytotoxic ones. Copper-mediated beads coated with an iron-mediated gel layer were more stable and had reduced cytotoxicity. The resulting polymeric structures had differing morphology, physical properties and cytotoxicity, which support their use in several applications, including biomedicine, agriculture and bioremediation.

GRAPHICAL ABSTRACT

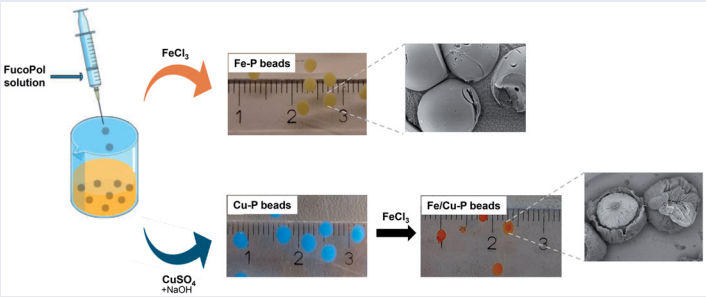

ARTICLE HISTORY
Received 1 August 2019
Accepted 6 November 2019

KEYWORDS
FucoPol; hydrogel beads; cytotoxicity

1. Introduction

Hydrogels are three-dimensional, hydrophilic, polymeric networks, with chemical or physical cross-links, which can be cast into various shapes and retain high amounts of water or biological fluids[1, 2]. The water retention properties of hydrogels are dependent on the polymers' composition and are mainly due to the presence of hydrophilic groups (e.g., carboxyl, hydroxyl). The swelling degree is also dependent on the cross-link density and nature[2]. Hydrogels have highly porous structures, with soft and elastic mechanical characteristics, which make their properties similar to those of biological tissues[2, 3].

Polysaccharides, due to their hydrophilic nature, together with their non-toxicity and biodegradability, are especially suitable for the preparation of hydrogels for different kinds of applications[3–5]. Cation-mediated gelation of negatively charged polysaccharides is frequently used to obtain polysaccharide hydrogels, in which gelation occurs through the linkage of polymer chains mediated by ions[5, 6]. The gelation mechanism involves the interaction of cations (e.g., calcium, copper, iron) with the polymers' negatively charged residues, resulting in ionic crosslinks between different polymer chains[5, 7]. Several natural polysaccharides, including alginate[3, 8], carrageenan[9], gellan gum[10, 11] and pectin[12] were used for the preparation of cation-mediated hydrogels.

Polysaccharide hydrogel beads can be obtained through ionotropic gelation by adding dropwise the polymeric solution, through a needle, into an aqueous solution containing polyvalent cations (e.g., Ca^{2+}, Cu^{2+}, Al^{3+})[13, 14]. The particles thus obtained have the rigidity of a soft solid conferred by the gel network and are permeable to small molecules and ions. Given these properties, polysaccharide hydrogel

CONTACT Filomena Freitas a4406@fct.unl.pt UCIBIO-REQUIMTE, Chemistry Department, Faculty of Sciences and Technology, Universidade NOVA de Lisboa, Campus da Caparica, Caparica, 2829–516, Portugal; Alexandra R Fernandes ma.fernandes@fct.unl.pt UCIBIO, Departamento Ciências da Vida, Faculdade de Ciências e Tecnologia, Universidade NOVA de Lisboa, Campus da Caparica, Caparica, 2829–516, Portugal.
Color versions of one or more of the figures in the article can be found online at www.tandfonline.com/gpom.
© 2019 Taylor & Francis Group, LLC

beads find applications ranging from biomedicine and food, to biotechnology and environmental technology[14–18].

FucoPol is a high molecular weight (1.7×10^6–5.8×10^6 Da) fucose-containing polysaccharide secreted by the bacterium *Enterobacter* A47 (DSM 23139)[19, 20]. FucoPol's repeating unit is a hexamer with two fucose, two galactose, one glucose and one glucuronic acid residues, corresponding to a molar ratio of 2.0:1.3:0.9:0.5[20, 21]. The main chain is composed of two α-(1,4)-linked fucose residues and a β-linked glucose residue, being one of the fucose residues branched at position 3. The branches are composed of 2 galactose and a glucuronic acid residue, with the terminal galactose residue pyruvated at positions 4 and 6. It also contains acyl groups (succinyl, pyruvyl and acetyl) that account for up to 22 wt% of the polymer's weight[20, 21]. The presence of glucuronic acid, as well as the acyl substituents succinyl and pyruvyl, confer the polymer an anionic character[21].

FucoPol forms viscous solutions with a shear thinning behaviour[22], has film-forming capacity and emulsion forming and stabilizing capacity[20, 21]. In addition, it was used for microencapsulation of bioactive compounds by spray drying[23]. It was also employed as a coating material for iron oxide magnetic nanoparticles and tested for human antibody purification[24] and for cell labeling by Magnetic Resonance Imaging[25].

FucoPol's ability to form gels has never been assessed, but the polymer's polyanionic character and high molecular weight has driven the interest on testing this valuable property. Therefore, in this study, the gel-forming capacity of FucoPol was studied, particularly in the presence of metal cations. Different salts were tested, including mono-, di- and trivalent metal cations, and the ones that resulted in the formation of a gel were tested for the preparation of beads. FucoPol gel beads were characterized in terms of physical-chemical properties, morphology, stability in aqueous solution, metal release and cytotoxicity.

2. Experimental

2.1. Screening of cations for metal induced gelation of FucoPol

Salts of several metal cations were tested, including monovalent (NaCl, KCl), divalent ($CaC1_2$, $MgSO_4$, $CuSO_4$, $ZnSO_4$) and trivalent ($FeCl_3$) cations. A FucoPol solution (10 g L^{-1}) was prepared by dissolving the polymer in deionized water and stirring for 1 h, at room temperature (25 °C). The gelation ability of the polymer was assessed according to the procedure described by Shimada et al.[26] with slight modifications. Briefly, 10 mg of each salt was dissolved in 1 mL of either NaOH 2 M (alkaline conditions) or deionized water (neutral conditions). Then, a volume of 4 mL of the FucoPol solution was mixed with the salt solutions.

2.2. Preparation of FucoPol hydrogel beads

A FucoPol solution (10 g L^{-1}) was prepared as described above and used for the preparation of the metal-FucoPol hydrogel beads. For the preparation of iron(III)-FucoPol beads (Fe–P beads), 1 mL of the FucoPol solution was dripped into 30 mL of an aqueous $FeCl_3$ solution (1.3×10^{-5} mM) through a needle with a 0.6 mm diameter. The mixture was kept under stirring (300 rpm), at room temperature (25 °C), for 30 minutes. Then, for removal of the unreacted crosslinker, the beads were washed with deionized water (30 mL; 4 times) until the pH was 6.5–7.5, and the conductivity was below 10 μS cm^{-1}.

For preparation of the copper(II)-FucoPol beads (Cu–P beads), 50 mg of $CuSO_4$ dissolved in 1 mL deionized water were mixed with 2 mL of the FucoPol solution. The resulting solution was dripped into 30 mL of a NaOH 2 M through a needle with a 0.6 mm diameter. The mixture was kept under stirring (300 rpm) at room temperature (25 °C). The Cu–P beads were removed from the solution 2 min after being formed and placed in deionized water for removal of unreacted NaOH and $CuSO_4$. The beads were washed 4 times with deionized water (30 mL) until reaching neutral pH and a conductivity value below 10 μS cm^{-1}. Iron(III)/Cu(II)-FucoPol beads (Fe/Cu–P beads) were obtained by transferring Cu–P beads, prepared as described above, into an aqueous $FeCl_3$ solution (1.3×10^{-5} mM). The beads were kept under stirring for 15 min (at 300 rpm).

2.3. Characterization of the beads

The metal-FucoPol beads were characterized in terms of their morphology (shape and size) by scanning electron microscopy (SEM), and color. SEM was performed with a Tabletop Microscope TM3030 (Hitachi in high technologies, America). Hydrated samples were observed at low temperature (–4 °C) with a magnification in the range of 30–1200×. The dried beads, obtained by freeze-drying the hydrogel beads, were analyzed by fourier transform infrared spectroscopy (FTIR) and thermogravimetric analysis (TGA). FTIR analysis was conducted with a Perkin-Elmer Spectrum two spectrometer. The spectra were recorded between 400 and 4000 cm^{-1} resolution with 10 scans, at room temperature. TGA was performed using a thermogravimetric equipment Labsys EVO (Setaram, France). The samples were placed in aluminum crucibles and analyzed in the temperature range between 25 and 500 °C, at 10 °C·min^{-1}. For quantification of the beads' metal content, they were placed in deionized water and hydrolyzed with 10% (v/v) trifluoracetic acid (TFA), at 120 °C, for 4 h. The samples were filtered (0.45 μm nylon; WHATMAN) and their content in iron and copper was determined by Inductively coupled plasma – atomic emission spectroscopy (ICP-AES) (Horiba Jobin-Yvon, France, Ultima model) equipped with a 40.68 MHz RF generator, Czerny-Turner monochromator with 1.00 m (sequential), autosampler AS500 and Concomitant Metals Analyzer (CMA).

2.4. Metal release from the FucoPol beads

The metal release from the FucoPol beads was evaluated in different aqueous media: deionized water, physiological

serum (NaCl 0.9%, w/v), simulated gastric fluid (SGF) without pepsin (NaCl 30 mM, HCl 0.3% (v/v), pH 1.2 ± 0.1), simulated intestinal fluid (SIF) without pancreatin (KH_2PO_4 50 mM, NaOH 0.015 N, pH 6.8 ± 0.1), phosphate-buffered saline (PBS, KH_2PO_4 1 mM, Na_2HPO_4 3 mM, NaCl 155 mM, KCl 30 mM, pH 7.4) and cell culture medium Dulbecco's Modified Eagle Medium (DMEM, ThermoFisher Scientific, Waltham, Massachusetts, USA) supplemented with 10% (v/v) heat inactivated fetal bovine serum (FBS, ThermoFisher Scientific) and a mixture of 100 U/mL penicillin and 100 µg/mL streptomycin (ThermoFisher Scientific). To evaluate the metal release over time in each solution, FucoPol beads were weighed (150 mg Cu–P, 100 mg Fe–P or 30 mg Fe/Cu–P beads), placed in 30 mL of each medium and kept at room temperature (25 °C) for 48 h, in an orbital shaker, at 150 rpm. Metal quantification was performed by ICP-AES, as described above. This test was also performed at 37 °C for DMEM-FBS. Results were normalized to time 0 h.

2.5. Biological assays

2.5.1. Cell culture

Normal human primary dermal fibroblasts, HPDFs; ovarian carcinoma cell line, A2780; breast adenocarcinoma cell line, MCF-7; lung adenocarcinoma cell line, A549; and chronic myeloid leukemia cell line, K562 (ATCC, Manassas, Virginia, USA) were used. A549 cell line was cultured in DMEM-FBS; MCF-7, HPDFs and K562 were cultured in DMEM-FBS supplemented with 1% (v/v) MEM (Minimum Essential Media) non-essential amino acids (ThermoFisher Scientific) and A2780 cell line was cultured on RPMI-1640 medium (ThermoFisher Scientific) supplemented with 10% FBS and a mixture of 100 U/mL penicillin and 100 mg/mL streptomycin[27, 28]. All cell cultures were maintained at 37 °C, 5% (v/v) CO_2, 99% (v/v) relative humidity.

2.5.2. Cytotoxicity via MTS assay

Cytotoxicity analysis of FucoPol in normal and tumor cells (HPDFs, A2780, A549, K562 and MCF-7) was performed as previously described by Fernandes et al.[29]. Briefly, cells were seeded in 96 well plates at a density of 0.75×10^4 cells per well. The culture medium was removed 24 h after seeding and replaced with fresh DMEM-FBS containing FucoPol at concentrations between 0 and 500 µg mL^{-1}. Two controls were used in each experiment, one without supplementation of FucoPol and another for assessing FucoPol interference in the MTS assay using an identical 96 well plate without cells. Cell viability was assessed after 48 h incubation using the CellTiter 96® AQueous One Solution Cell Proliferation Assay Kit (Promega, Madison, EUA), according to the manufacturer's instructions. After cell incubation with FucoPol, the supernatant was removed and replaced by fresh medium supplemented with 20% (v/v) MTS solution. After an incubation period of 45 min at 37 °C, 5% (v/v) CO_2 and 99% (v/v) relative humidity, the absorbance at 490 nm was determined using a Tecan Infinite F200 Microplate Reader (Tecan, Männedorf, Switzerland). The obtained data was normalized relative to control samples to obtain cell viability (%) for each FucoPol concentration using the following equation:

$$\text{cell viability (\%)} = \frac{\text{Abs}_{490}\ \text{with cells} - \text{Abs}_{490}\ \text{without cells}}{\text{Abs}_{490}\ \text{control with cells} - \text{Abs}_{490}\ \text{control without cells}} \times 100 \quad (1)$$

2.5.3. Cytotoxicity via trypan blue

The cytotoxicity of FucoPol and FucoPol beads was also evaluated on K562 cell line using the Trypan Blue Exclusion method according to Strobber[30]. Cells were seeded on a 24-well plate at a density of 2.5×10^4 cells per well in DMEM-FBS supplemented with increasing concentrations of FucoPol (0–500 µg mL^{-1}) or FucoPol beads (3–4 beads were used in each well, corresponding to a mass of 40, 150 or 17 mg for the Fe–P, Cu–P or Fe/Cu–P beads, respectively). Control assays were also conducted. After 48 h incubation, the cellular suspension was mixed with 0.4% (w/v) Trypan Blue (ThermoFisher Scientific) in a 4:1 proportion (cells: trypan blue). The mixture was loaded on a hemocytometer (Hirschmann, Eberstadt, Germany) and the number of viable cells was counted in an Olympus CXX41 inverted microscope (Tokyo, Japan).

3. Results and discussion

3.1. Screening of cations for metal induced gelation of FucoPol

As shown in Table 1 and Figure 1, under neutral pH conditions, no gelation of FucoPol was observed, except in the presence of the trivalent cation Fe^{3+}. Under the conditions tested, upon mixing the polymer solution with the $FeCl_3$ solution, a strong gel was formed. For all other salts tested, no significant changes in the mixtures were observed (Figure 1, upper image). However, under alkaline conditions, gel formation was observed in the presence of the divalent cation Cu^{2+} (Figure 1, lower image). No changes were observed in the presence of the tested monovalent cations (Na^+ and K^+) or the divalent cation Zn^{2+}, while Ca^{2+} lead to the formation of a white precipitate (Table 1).

Since among the tested salts, $FeCl_3$ and $CuSO_4$ resulted in the formation of the strongest gels, these salts were selected to prepare FucoPol gel beads.

Table 1. Results obtained with the different tested methods.

Salt	Deionized water	NaOH 2 M
NaCl	(–)	(–)
KCl	(–)	(–)
$CaCl_2$	(–)	pp
$MgSO_4$	(–)	(–)
$CuSO_4$	(–)	(++)
$ZnSO_4$	(–)	(–)
$FeCl_3$	(++)	x

(–): no alteration; pp: formation of a precipitate; (+): weak gel formation; (++): strong gel formation; x: not tested

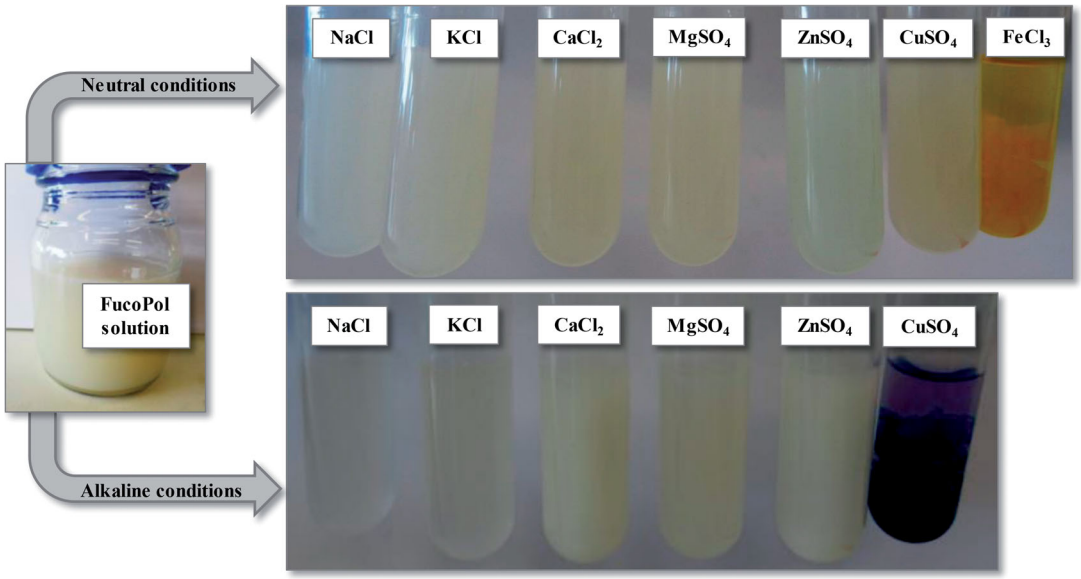

Figure 1. Original FucoPol solution and the results of the tests made to assess gel formation with different salts, under neutral conditions (upper image) or alkaline conditions (lower image).

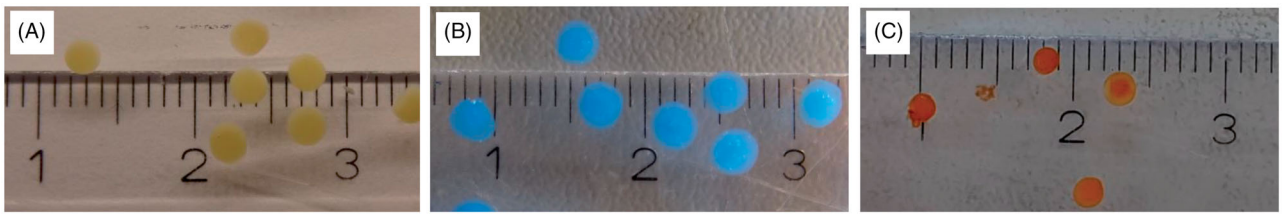

Figure 2. FucoPol hydrogel beads: (A) Fe–P beads; (B) Cu–P beads; (C): Fe/Cu–P beads.

3.2. FucoPol gel beads

Given the ability of FucoPol to gel under neutral pH conditions, Fe–P beads were prepared by dripping the polymer solution into a $FeCl_3$ solution. Yellow spherical gel beads with 2.0–3.0 mm diameter were spontaneously formed (Figure 2A). The beads had an average mass of 7.90 ± 0.002 mg, with a water content of 98.60 ± 0.26 wt% (Table 2). Their iron content was 11.54 ± 1.09 µg per bead, thus corresponding to 0.15 ± 0.01 wt% of the beads' mass. Therefore, the beads' metal-to-polymer ratio was only 0.12 $mg_{Fe}/mg_{FucoPol}$. The formed structures were stable, withstanding over 6 months in deionized water at room temperature (25 °C), without any visible alteration of their shape, size or color.

The Cu–P beads were prepared under alkaline conditions by dripping the polymer solution containing $CuSO_4$ into a NaOH 2 M solution. The beads were also spherical but had a blue color and were larger than the Fe–P beads, displaying a mean diameter of 3.0–4.0 mm (Table 2, Figure 2B). Concomitantly, the beads had a considerably higher mass (50.59 ± 0.006 mg) than the Fe–P beads and a higher water content (99.84 ± 0.06 wt%) (Table 2). The beads had a copper content of 134.50 ± 29.63 µg per bead, which corresponded to 0.27 ± 0.06 wt% of their mass. Comparing to the Fe–P, the Cu–P beads were rather fragile, swallowing and disintegrating after 24 h in deionized water at room temperature (25 °C). This lower stability may be related to the fact that the metal-to-polymer ratio was considerable higher (1.66 $mg_{Cu}/mg_{FucoPol}$) than that of the Fe-P beads (0.12 $mg_{Fe}/mg_{FucoPol}$). The low polymer content of the beads has resulted probably in a weaker gel network.

Table 2. Main characteristics of the metal-FucoPol beads.

Parameter	Fe–P	Cu–P	Fe/Cu–P
Shape	Spherical	Spherical	Spherical
Color	Yellow	Blue	Dark orange
Diameter (mm)	2.0–3.0	3.0–4.0	1.5–2.0
Mass (mg)	7.90 ± 0.002	50.59 ± 0.006	9.28 ± 0.002
Water content (wt%)	98.60 ± 0.26	99.84 ± 0.06	99.27 ± 0.47
Metal content (µg/bead)			
Copper	–	134.50 ± 29.63	118.33 ± 20.54
Iron	11.54 ± 1.09	–	11.84 ± 3.21

Fe–P: iron-FucoPol; Cu–P: copper-FucoPol; Fe/Cu–P: iron- and copper-FucoPol

In an attempt to obtain more stable copper containing beads, Cu–P beads were prepared and placed in a $FeCl_3$ solution. This strategy was successful since the resulting Fe/Cu–P beads were stable for over 15 days in deionized water, at room temperature. These beads had a dark orange color and were smaller than both the Fe–P and the Cu–P beads, with a mean diameter of 1.5–2.0 mm (Table 2, Figure 2C). They had a water content of 99.27 ± 0.47 wt%, similar to the Cu–P beads. The Fe/Cu–P beads had iron and copper contents of 11.84 ± 3.21 and 118.33 ± 20.54 µg/bead, respectively (Table 2), corresponding to metal-to-polymer ratios of 0.17 $mg_{Fe}/mg_{FucoPol}$ and 1.75 $mg_{Cu}/mg_{FucoPol}$, respectively. These results suggest that the Fe/Cu–P beads had a core

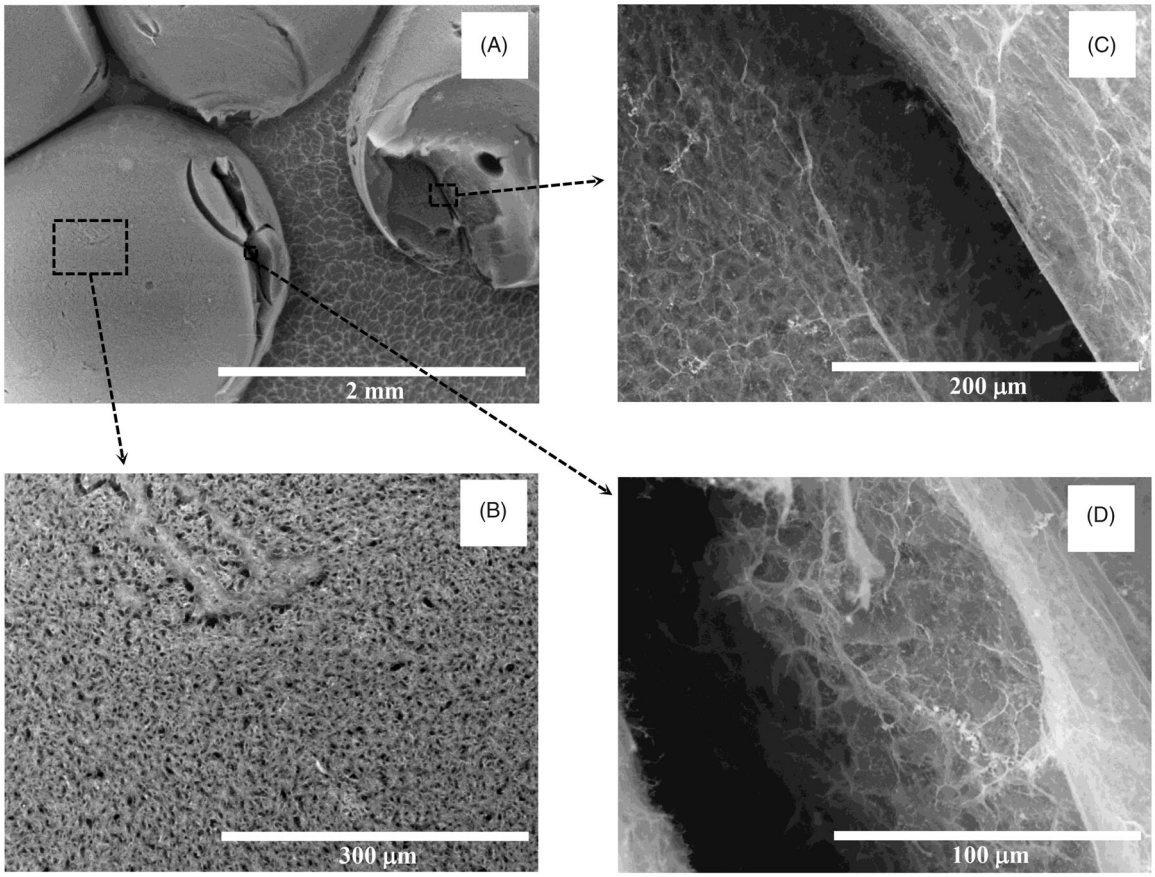

Figure 3. SEM images of hydrated Fe–P beads at a temperature of –4 °C.

made of Cu-mediated FucoPol gel, surrounded by an outer shell of Fe-mediated FucoPol gel that eventually stabilized the final Fe/Cu–P beads' structure.

3.3. FucoPol gel beads characterization

3.3.1. Morphology

The surface morphology of the prepared Fe–P and Fe/Cu–P hydrogel beads was observed by SEM (Figures 3 and 4). Given the fragility of the Cu–P beads, they disintegrated upon freezing, rendering their visualization by this technique not possible.

The Fe–P beads had a smooth surface but presented some fractures (Figure 3A). Upon magnification of a bead's smooth surface, a rather homogeneous porous structure was observed (Figure 3B). Moreover, different porous structures could be seen upon magnification of the fractured portions of the beads' surface (Figures 3C and 3D).

The Fe/Cu–P beads presented a much more complex structure, with an almost spherical internal core surrounded by an outer shell (Figures 4A and 4B). The core was attributed to an internal bead formed by gelation in the presence of copper, while the outer shell is envisaged to be formed when the Cu–P beads were placed in the $FeCl_3$ solution. Upon magnification, different structures could be observed. The inner core seemed to be more compact, presenting stretch marks emerging outwards from the center of the bead (Figure 4A.1). Upon a closer look (Figure 4B.1), the structure of the inner core was actually rough with pores of different shapes and sizes. The outer shell also presented striated and porous structures (Figure 4B.1) but was much less compact, as shown by their lacelike structure (Figures 4A.2 and 4B.2).

3.3.2. Fourier-transform infrared spectra analysis

FTIR analysis was carried out to understand the interaction between FucoPol's functional groups and the metal cations. As shown in Figure 5, the FTIR spectrum of Fe–P beads (full red line) mainly shows the bands characteristic of FucoPol (full gray line)[21] which is in accordance with the low metal-to-polymer ratio of the Fe-P gel beads (0.10 mg_{Fe}/$mg_{FucoPol}$). Nevertheless, it can be seen that the interaction of FucoPol with iron led to shifts of several absorption peaks, especially those attributed to the hydroxyl and carboxylate groups. The broad and intense band corresponding to the stretching frequencies of hydroxyl groups (O–H), observed at 3300 cm^{-1} for FucoPol (Figure 5-full gray line), was shifted to 3275 cm^{-1} in the Fe–P spectrum (Figure 5-full red line). The absorption peaks at 1722 and 1016 cm^{-1} that can be attributed to the C=O stretching of the carbonyl moieties found in the acyl substituents[21] and to C–O and C–C vibrations of the glycosidic bonds and pyranoid ring[31], respectively, were shifted to 1720 and 1023 cm^{-1}. The C–H stretching peak of CH_2 groups[32] appearing at 2925 cm^{-1} was also shifted to a lower wavenumber (2922 cm^{-1}). The peak at 1600 cm^{-1} and the absorption

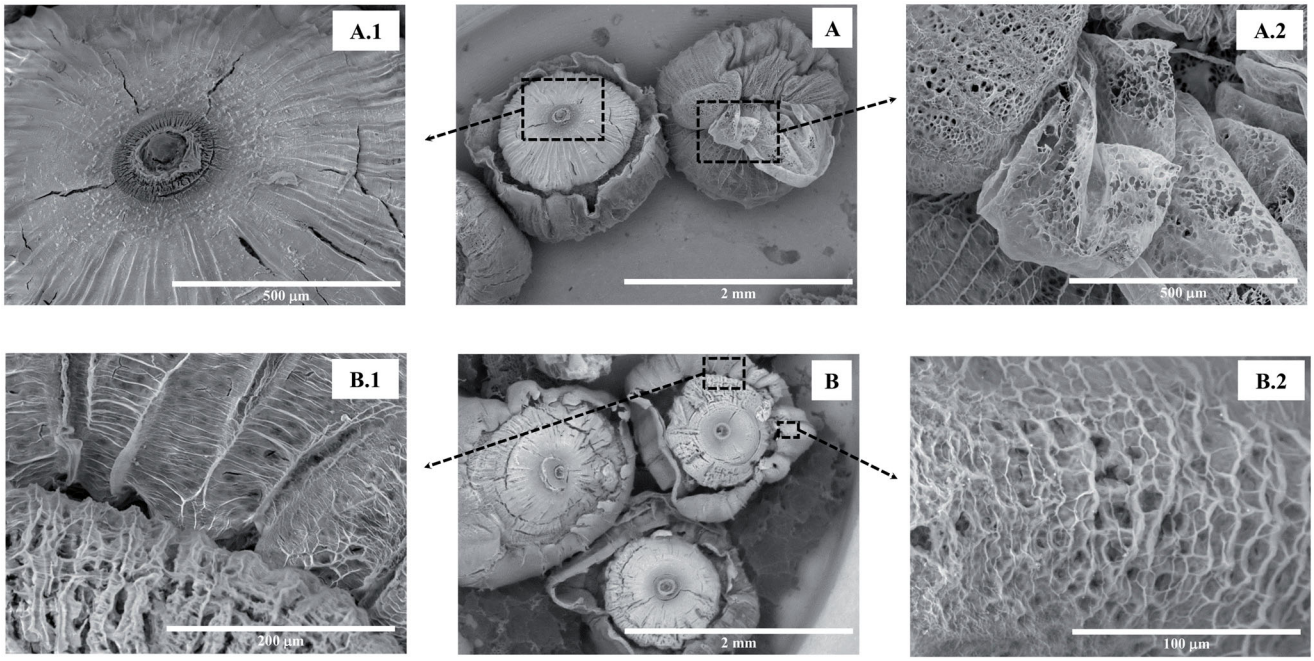

Figure 4. SEM images of hydrated Fe/Cu–P beads at a temperature of –4 °C.

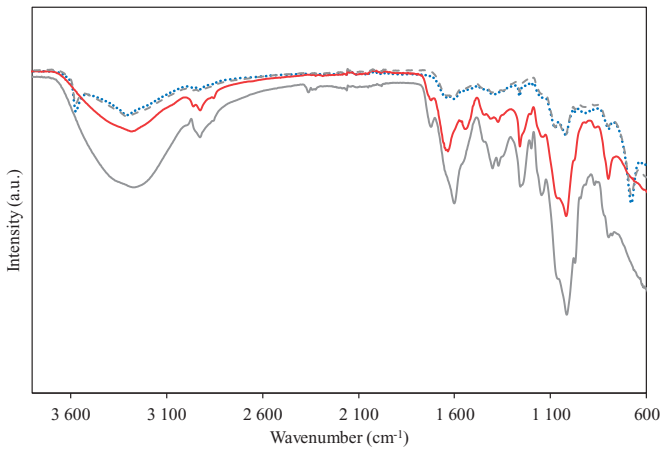

Figure 5. FTIR spectra of FucoPol (full gray line) and dried FucoPol gel beads: Fe–P (full red line), Cu–P (dotted line), Fe/Cu–P (dashed line).

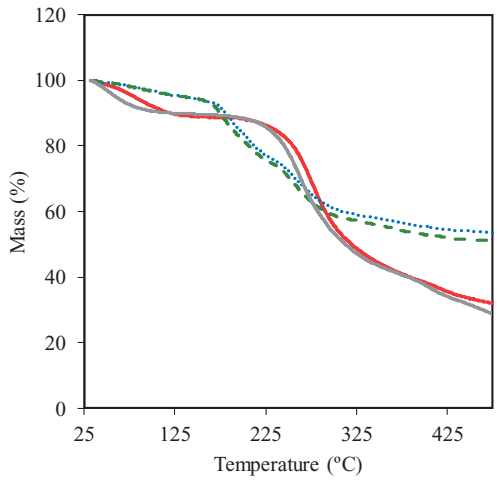

Figure 6. Thermogravimetric analysis of FucoPol (full gray line) and dried FucoPol gel beads: Fe–P (full red line), Cu–P (dotted line), Fe/Cu–P (dashed line)

region at 1370–1400 cm^{-1} that can be attributed to the asymmetric and symmetric stretching of carboxylates from glucuronic acid[31] were also shifted to 1635 cm^{-1} and 1380–1418 cm^{-1}, respectively. Similarly, the band at 1254 cm^{-1} that may also be attributed to the C–O–C vibration of acyls[33] was shifted to 1260 cm^{-1}.

Regarding the Cu–P and Fe/Cu–P beads, although the FTIR spectra shows the same main peaks (Figure 5-dotted and dashed lines, respectively) displayed by FucoPol, they are much less intense. This may be related to the high metal-to-polymer ratio of those beads. The main difference is that the peak appearing at 1722 cm^{-1} in FucoPol spectrum was is no longer observed in neither the Cu–P or the Fe/Cu–P beads spectra, suggesting that the carbonyl moieties found in the acyl substituents were involved in the interaction between the polymer chain and the metals. Moreover, two new peaks are observed at 3580 and 680 cm^{-1} in both copper-containing beads spectra, which may be indicative of the presence of $Cu(OH)_2$ formed upon exposure of Cu(II) to NaOH during the preparation of the beads. The peak at 3580 cm^{-1} may reflect stretching modes of the hydroxyl groups in $Cu(OH)_2$, while the peak at 680 cm^{-1} might correspond to the C–O stretching vibration of Cu^{2+} in $Cu(OH)_2$[34].

3.3.3. Thermogravimetric analysis

The thermal degradation curves of FucoPol and Fe–P beads (Figure 6) presented three mass loss regions. For FucoPol (full gray line) and the Fe–P beads (full red line), the first mass loss, of around 15%, was observed within 35–140°C and 35–150°C, respectively, and can be attributed to water evaporation[23]. The higher temperature range observed for

Table 3. Iron and/or copper release from the Fe–P, Cu–P and Fe/Cu–P beads in different media, after 24 h (all tests were performed at 25 °C, except in DMEM, for which experiments were conducted also at 37 °C).

Media	Fe–P beads [Fe] (mg L^{-1})	Cu–P beads [Cu] (mg L^{-1})	Fe/Cu–P beads [Fe] (mg L^{-1})	Fe/Cu–P beads [Cu] (mg L^{-1})
Water	0.00 ± 0.00	0.25 ± 0.06	0.01 ± 0.00	0.15 ± 0.03
NaCl 0.9%	0.01 ± 0.00	0.08 ± 0.02	0.00 ± 0.00	0.12 ± 0.02
PBS	0.18 ± 0.02	0.08 ± 0.02	0.01 ± 0.00	0.12 ± 0.02
SGF	*	*	*	*
SIF	0.19 ± 0.02	*	0.00 ± 0.00	0.03 ± 0.00
DMEM-FBS				
25 °C	0.00 ± 0.00	*	0.00 ± 0.00	0.02 ± 0.00
37 °C	0.00 ± 0.00	*	0.00 ± 0.00	0.98 ± 0.17

Fe–P: iron-FucoPol; Cu–P: copper-FucoPol; Fe/Cu–P: iron- and copper-FucoPol
*beads disintegration.

the Fe–P beads sample suggests that water is bound more strongly in the beads than in FucoPol. The largest mass loss (around 50%) occurred between 180 and 380 °C and is probably associated with the polysaccharide's side chains decomposition[35]. The third mass loss comprised a gradual weight loss observed above 380 °C that is probably associated with the polysaccharide' main-chain scission degradation[35]. Char yields of 24% and 25% were obtained for FucoPol and the Fe–P beads, respectively. These results show that the thermal properties of FucoPol were not significantly altered by the presence of iron in the Fe–P beads.

For the Cu–P and Fe/Cu–P beads (Figure 6, dotted and dashed lines, respectively), there was a gradual mass loss of around 11% between 35 and 170 °C, associated with water evaporation. The lower mass loss observed for these beads might be related with the considerably lower polymer content in the copper-containing beads. The largest mass losses occurred within 170–430 °C in which around 38% of the samples' mass was degraded, resulting in a final char yield of 51–53%. The higher char yield is probably related with the significantly higher metal content of the Cu–P and Fe/Cu–P beads.

3.4. Metal release from the FucoPol beads

The metal release from the FucoPol gel beads was evaluated in different aqueous solutions (Table 3) representing some biological contexts of *in vitro* studies (PBS and DMEM-FBS) or simulating human body environments after oral ingestion of the beads (SGF, SIF and physiological serum).

All beads disintegrated in SGF in only a few minutes after exposure to the medium (Table 3). However, the polymer was not degraded, suggesting the low pH of the medium (pH 1.2 ± 0.1) may have destabilized the gel structure, leading to bead disaggregation and, consequently, polymer dissolution. In all the other tested media, the beads kept their integrity, although in some cases they swelled, and their shape or size were altered.

Regarding the Fe–P beads, there was no significant iron release in water, physiological serum or DMEM-FBS (Table 3), and the beads remained unchanged during the 24 h of the assay. However, in PBS solution and SIF, the iron release was 0.18 ± 0.02 and 0.19 ± 0.02 mg/L, respectively, that correspond to only 3.7 and 3.9% of the beads' iron content. The iron release observed in PBS and SIF may be related to the solutions' pH that was around 6.8–7.4, while for deionized water and physiological serum it was 5.5–5.8. Moreover, the higher salts concentration of PBS and SIF compared to deionized water and the physiological serum may also have impacted on the release of iron from the beads. The presence of additional cations (K^+, Na^+) and anions (PO_4^{3-}, Cl^-) may have interfered on the interaction between the polymer chain and Fe^{3+}.

Considering the Cu–P beads, although their shape was maintained during the assays in water, physiological serum and PBS, they got progressively swelled over time. The beads released on average 0.25 ± 0.06 mg L^{-1} of copper in deionized water, while 0.08 ± 0.02 mg L^{-1} were released in physiological serum and PBS (Table 3). These values represent less than 2% of the beads' copper content. In SGF, DMEM-FBS and SIF, on the other hand, there was a gradual decrease of the beads' size, being totally disintegrated within a few minutes, 6 min and 24 min, respectively, thus releasing all their copper content into the media.

As for Fe/Cu–P beads, their shape was maintained during the assays in physiological serum, DMEM-FBS, PBS and SIF, and only disintegrated in SGF (Table 3). These results show that the iron-mediated gel layer formed over the copper-containing gel bead conferred stability to the beads, allowing them to withstand the presence of SIF and DMEM-FBS without the disintegration observed in those media for the single Cu-P beads. Moreover, there was no significant iron release from the beads in any of the tested media, while copper release was below 2% for most media (Table 3). The exception was DMEM-FBS, at 37 °C, in which a copper concentration of 0.98 ± 0.17 mg L^{-1} was detected, which corresponds to almost 8% of the beads' copper content. Since no copper release was noticed in DMEM-FBS at 25 °C, probably the higher temperature (37 °C) partially destabilized the gel structure and led to copper release in this medium. Indeed, in this assay, the beads appeared to be more translucent, thus indicating changes on their structure.

3.5. Biological evaluation

3.5.1. Cytotoxic evaluation of FucoPol

The antiproliferative effect of FucoPol in a colorectal carcinoma cell line, HCT116, was previously described by Palma et al.[25]. A reduction of 30% in HCT116 cell viability was observed after exposure of cells to FucoPol at a concentration of 138 µg/mL for 48 h[25]. In this study, FucoPol effect was evaluated in other tumor epithelial cell lines (including ovarian carcinoma cell line, A2780, lung adenocarcinoma cell line, A549, breast adenocarcinoma cell line, MCF-7, and in a chronic myelogenous leukemia cell line, K562) and in normal human primary dermal fibroblasts, HPDFs.

Cell viability after 48 h of treatment with increasing concentrations of FucoPol was measured using the MTS assay, where the production of formazan is proportional to cell viability. No loss of HPDFs, A549, MCF-7, and K562 cell viability for concentrations of FucoPol up to 500 µg/mL (Figure 7). In contrast, the A2780 tumor cell line showed to

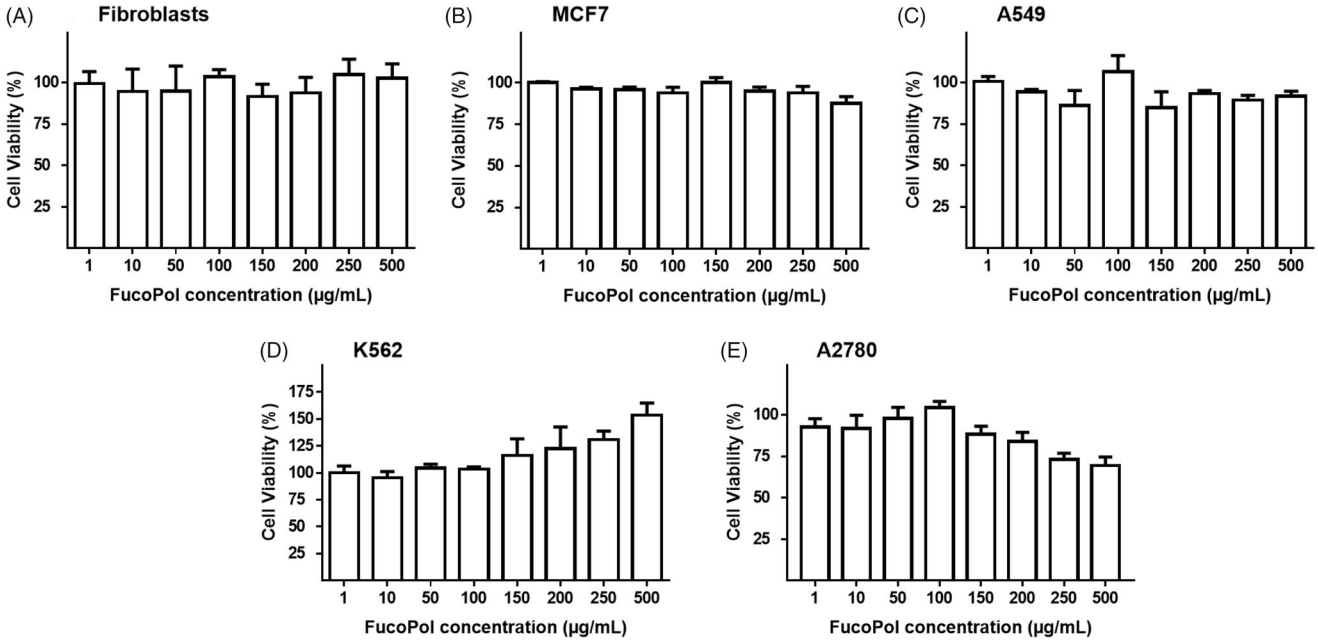

Figure 7. Cytotoxicity of FucoPol in normal human dermal fibroblasts (A), breast adenocarcinoma cell line MCF-7 (B), lung adenocarcinoma cell line A549 (C), Chronic myelogeneous leukemia cell line K562 (D) and ovarian carcinoma cell line A2780 (E). Cells were treated with increasing concentrations of polymer for 48 h and cell viability was determined by the MTS assay. Data was normalized against the control (cells grown without polymer) and expressed as average ± standard error mean of three independent assays.

be more sensitive, compared to the other cell lines, with a reduction of cell viability of 30.5% for a FucoPol concentration of 500 µg/mL (Figure 7E). Considering these results and also those reported previously, FucoPol can be considered a safe polymer for further biological studies.

3.5.2. Cytotoxic evaluation of FucoPol beads

Considering that no loss of viability was observed with FucoPol in K562, this cell line was chosen for testing the Fe–P, Cu–P and Fe/Cu–P hydrogel beads using the Trypan-blue exclusion method[30]. For comparison, the viability of free FucoPol was also evaluated in K562 cell line using the same. In accordance with results obtained in Figure 7D, no alterations of viability were observed when K562 cells were exposed to 500 µg/mL FucoPol (Figure 8).

As evidenced in Figure 9, the Fe–P beads are not cytotoxic for K562 cells during the 48 h of incubation period since a cell viability of 94.7 ± 8.3% was obtained. These results agree with the fact that no iron release was observed from the beads upon exposure to DMEM-FBS medium at 37 °C (as shown in Table 3). Incubation of K562 cells with the Cu-P beads resulted in a 55% cell viability decrease (Figure 9), that might be correlated with the beads' disintegration with the concomitant release of their copper content. Since no cell viability loss was observed in the presence of FucoPol (Figure 8), the reduced K562 cell viability observed (Figure 9) can be attributed to the release of copper to the medium from the Cu–P beads.

In fact, each bead had a copper content of 134.50 ± 29.63 µg, thus corresponding to a concentration of around 201.75 ± 177.78 µg/mL in each well. According to Ruiz et al.[36], exposure to copper concentrations above 100 mM (i.e., 6.35 µg mL^{-1}) does not induce K562 cells

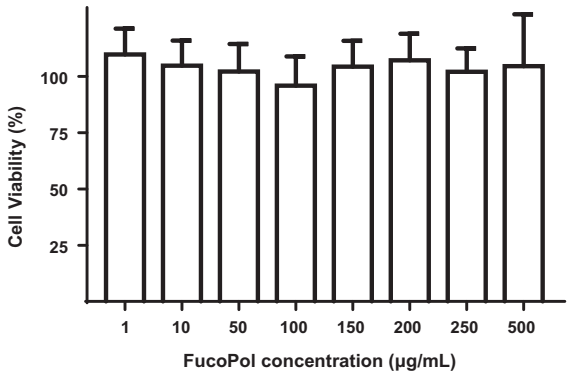

Figure 8. Viability accessed using Trypan Blue exclusion method of K562 cells treated with FucoPol. Cells were treated with increasing concentrations of polymer for 48 h and cell viability was determined. Data was normalized against the control (cells grown without polymer) and expressed as average ± standard error mean of three independent assays.

death but affects cell differentiation and proliferation. In this study, K562 cells were exposed to a considerably higher copper concentrations that led to the observed reduction of the cells' viability (Figure 9).

Concerning the Fe/Cu–P beads, there was a slight decrease in K562 cells viability of 21.4% that might be also correlated with the release of copper from the respective beads. Although the beads did not disintegrate, they released copper upon cultivation in DMEM-FBS medium (Table 3), resulting in a copper concentration of approximately 72.7 ± 12.6 µg/mL in each well, which is already cytotoxic[36].

The results presented here show the antiproliferative potential of Cu–P and Fe/Cu–P beads per se (particularly the first ones) in K562 cells, thus supporting the future incorporation of Imatinib in those beads towards increasing this antiproliferative effect and their potential for chronic myeloid leukemia (CML) therapy[37]. The Fe–P beads, on

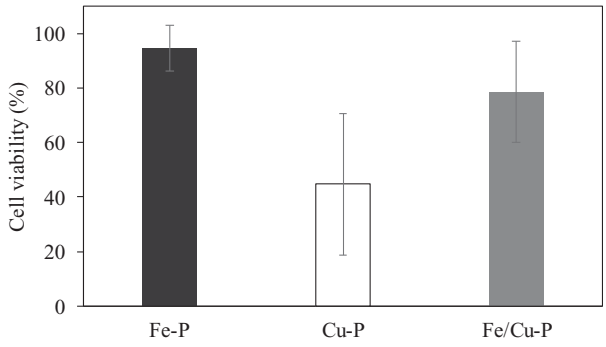

Figure 9. Viability of K562 cells in the presence of 150 mg Fe–P (black bars), Cu–P (white bar) and Fe/Cu–P (gray bar) beads after 48 h incubation. Viability was accessed using the Trypan Blue exclusion method, normalized to the control (cells grown in non-supplemented medium) and represented as the average ± SEM of three independent assays.

the other hand, posed no cytotoxicity under the conditions tested, which supports their potential use as drug delivery carriers.

4. Conclusions

This study demonstrates for the first time the potential of the fucose-rich polysaccharide FucoPol for the development of polymeric structures by its cation-mediated gelation. Iron(III) and/or copper(II) were used to obtain FucoPol hydrogels with different valuable properties that envisage their use in distinct areas. The iron-containing gel beads, given their stability and non-cytotoxicity, may be used, for example, for the development of drug delivery carriers, while the copper-containing gel beads may find applicability in CML therapy due to their antiproliferative action.

Funding

This work was supported by the Unidade de Ciências Biomoleculares Aplicadas (UCIBIO) and LEAF-Linking Landscape, Environment, Agriculture and Food, which are financed by national funds from FCT/MEC [UID/Multi/04378/2019 and PEst-OE/AGR/UI0245/2014, respectively] and co-financed by the ERDF, under the PT2020 Partnership Agreement [POCI-01-0145-FEDER-007728 and POCI-01-0145-FEDER – 007265, respectively]. FCT/MCTES is also acknowledged for scholarships SFRH/BD/140829/2018 and SFRH/BPD/124612/2016.

ORCID

Letícia Fialho http://orcid.org/0000-0002-3782-157X
Diana Araújo http://orcid.org/0000-0003-4376-6471
Vitor D. Alves http://orcid.org/0000-0002-4117-5582
Filomena Freitas http://orcid.org/0000-0002-9430-4640

References

[1] Coviello, T.; Matricardi, P.; Marianecci, C.; Alhaique, F. Polysaccharide Hydrogels for Modified Release Formulations. *J. Control. Release.* **2007**, *119*, 5–24. DOI: 10.1016/j.jconrel.2007.01.004.

[2] Biondi, M.; Borzacchiello, A.; Mayol, L.; Ambrosio, L. Nanoparticle-Integrated Hydrogels as Multifunctional Composite Materials for Biomedical Applications. *Gels.* **2015**, *1*, 162. DOI: 10.3390/gels1020162.

[3] Marković, D.; Zarubica, A.; Stojković, N.; Vasić, M.; Cakić, M.; Nikolić, G. Alginates and Similar Exopolysaccharides in Biomedical Applications and Pharmacy: Controlled Delivery of Drugs. *Adv. Techn.* **2016**, *5*, 39. DOI: 10.5937/savteh1601039M.

[4] Camponeschi, F.; Atrei, A.; Rocchigiani, G.; Mencuccini, L.; Uva, M.; Barbucci, M. New Formulations of Polysaccharide-Based Hydrogels for Drug Release and Tissue Engineering. *Gels.* **2015**, *1*, 3. DOI: 10.3390/gels1010003.

[5] Pasqui, D.; De Cagna, M.; Barbucci, R. Polysaccharide-Based Hydrogels: The Key Role of Water in Affecting Mechanical Properties. *Polymers.* **2012**, *4*, 1517. DOI: 10.3390/polym4031517.

[6] Burey, P.; Bhandari, B. R.; Howes, T.; Gidley, M. J. Hydrocolloid Gel Particles: Formation, Characterization, and Application. *Crit. Rev. Food Sci. Nutr.* **2008**, *48*, 361. DOI: 10.1080/10408390701347801.

[7] Rodrigues, J. R.; Lagoa, R. Copper Ions Binding in Cu-Alginate Gelation. *J. Carbohydr. Chem.* **2006**, *25*, 219. DOI: 10.1080/07328300600732956.

[8] Yamamoto, K.; Yuguchi, Y.; Stokke, B. T.; Sikorski, P.; Bassett, D. C. Local Structure of Ca^{2+} Alginate Hydrogels Gelled via Competitive Ligand Exchange and Measured by Small Angle X-Ray Scattering. *Gels.* **2019**, *5*, 3. DOI: 10.3390/gels5010003.

[9] Running, C. A.; Falshaw, R.; Janaswamy, S. Trivalent Iron Induced Gelation in Lambda-Carrageenan. *Carbohydr. Pol.* **2012**, *87*, 2735. DOI: 10.1016/j.carbpol.2011.11.018.

[10] Funami, T.; Noda, S.; Nakauma, M.; Ishihara, S.; Takahashi, R.; Al-Assaf, S.; Ikeda, S.; Nishinari, K.; Phillips, G. O. Molecular Structures of Gellan Gum Imaged with Atomic Force Microscopy in Relation to the Rheological Behavior in Aqueous Systems in the Presence or Absence of Various Cations. *J. Agric. Food Chem.* **2008**, *56*, 8609.DOI: 10.1021/jf8007713.

[11] Picone, C. S. F.; Cunha, R. L. Influence of pH on Formation and Properties of Gellan Gels. *Carbohydr. Pol.* **2011**, *84*, 662. DOI: 10.1016/j.carbpol.2010.12.045.

[12] Fraeye, I.; Duvetter, T.; Doungla, E.; Van Loey, A.; Hendrickx, M. Fine-Tuning the Properties of Pectin Calcium Gels by Control of Pectin Fine Structure, Gel Composition and Environmental Conditions. *Trends Food Sci. Technol.* **2010**, *21*, 219–e228. DOI: 10.1016/j.tifs.2010.02.001.

[13] Swamy, B. Y.; Yun, Y. S. *In Vitro* Release of Metformin from Iron(III) Cross-Linked Alginate–Carboxymethyl Cellulose Hydrogel Beads. *Int. J. Biol. Macromol.* **2015**, *77*, 114. DOI: 10.1016/j.ijbiomac.2015.03.019.

[14] Perez-Moral, N.; Gonzalez, M. C.; Parker, R. Preparation of Iron-Loaded Alginate Gel Beads and Their Release Characteristics under Simulated Gastrointestinal Conditions. *Food Hydrocoll.* **2013**, *31*, 114. DOI: 10.1016/j.foodhyd.2012.09.015.

[15] Banerjee, A.; Nayak, D.; Lahiri, S. A New Method of Synthesis of Iron Doped Calcium Alginate Beads and Determination of Iron Content by Radiometric Method. *Biochem. Eng. J.* **2007**, *33*, 260. DOI: 10.1016/j.bej.2006.11.005.

[16] Rayment, P.; Wright, P.; Hoad, C.; Ciampi, E.; Haydock, D.; Gowland, P.; Butler, M. F. Investigation of Alginate Beads for Gastro-Intestinal Functionality, Part 1: *In Vitro* Characterisation. *Food Hydrocoll.* **2009**, *23*, 816–e822. DOI: 10.1016/j.foodhyd.2008.04.011.

[17] Rosales, E.; Iglesias, O.; Pazos, M.; Sanromán, M. A. Decolourisation of Dyes under electro-Fenton Process Using Fe Alginate Gel Beads. *J. Hazard. Mat.* **2012**, *213–214*, 369. DOI: 10.1016/j.jhazmat.2012.02.005.

[18] Valenzuela, C.; Hernández, V.; Morales, M. S.; Neira-Carrillo, A.; Pizarro, F. Preparation and Characterization of Heme Iron-Alginate Beads. *LWT – Food Sci. Technol.* **2014**, *59*, 1283–1289. DOI: 10.1016/j.lwt.2014.04.030.

[19] Alves, V. D.; Freitas, F.; Torres, C. A. V.; Cruz, M.; Marques, R.; Grandfils, C.; Gonçalves, M. P.; Oliveira, R.; Reis, M. A. M. Rheological and Morphological Characterization of the Culture

Broth during Exopolysaccharide Production by *Enterobacter* sp. *Carbohydr. Pol.* **2010**, *81*, 758. DOI: 10.1016/j.carbpol.2010.03.048.

[20] Freitas, F.; Alves, V. D.; Gouveia, A. R.; Pinheiro, C.; Torres, C. A. V.; Grandfils, C.; Reis, M. A. M. Controlled Production of Exopolysaccharides from *Enterobacter* A47 as a Function of Carbon Source with Demonstration of Their Film and Emulsifying Abilities. *Appl. Biochem. Biotechnol.* **2014**, *172*, 641. DOI: 10.1007/s12010-013-0560-0.

[21] Freitas, F.; Alves, V. D.; Torres, C. A. V.; Cruz, M.; Sousa, I.; Melo, M. J.; Ramos, A. M.; Reis, M. A. M. Fucose-Containing Exopolysaccharide Produced by the Newly Isolated *Enterobacter* Strain A47 DSM 23139. *Carbohydr. Polym.* **2011**, *83*, 159. DOI: 10.1016/j.carbpol.2010.07.034.

[22] Torres, C. A. V.; Ferreira, A. R. V.; Freitas, F.; Reis, M. A. M.; Coelhoso, I.; Sousa, I.; Alves, V. D. Rheological Studies of the Fucose-Rich Exopolysaccharide FucoPol. *Int. J. Biol. Macromol.* **2015**, *79*, 611. DOI: 10.1016/j.ijbiomac.2015.05.029.

[23] Lourenço, S. C.; Torres, C. A. V.; Nunes, D.; Duarte, P.; Freitas, F.; Reis, M. A. M.; Fortunato, E.; Martins, M. M.; da Costa, L. B.; Alves, V. D. Using a Bacterial Fucose-Rich Polysaccharide as Encapsulation Material of Bioactive Compounds. *Int. J. Biol. Macromol.* **2017**, *104*, 1099. DOI: 10.1016/j.ijbiomac.2017.07.023.

[24] Dhadge, V. L.; Morgado, P. I.; Freitas, F.; Reis, M. A. M.; Azevedo, A.; Aires-Barros, R.; Roque, A. C. A. An Extracellular Polymer at the Interface of Magnetic Bioseparations. *J. R Soc. Interface.* **2014**, *11*, 20140743. DOI: 10.1098/rsif.2014.0743.

[25] Palma, S. I. C. J.; Rodrigues, C. A. V.; Carvalho, A.; Morales, M. d P.; Freitas, F.; Fernandes, A. R.; Morales, M. P.; Cabral, J. M. S.; Roque, A. C. A. A Value-Added Exopolysaccharide as a Coating Agent for MRI Nanoprobes. *Nanoscale.* **2015**, *7*, 14272. DOI: 10.1039/C5NR01979F.

[26] Shimada, A.; Nakata, H.; Nakamura, I. Acidic Exopolysaccharide Produced by *Enterobacter* sp. *J. Ferment. Bioeng.* **1997**, *84*, 113. DOI: 10.1016/S0922-338X(97)82538-X.

[27] Sutradhar, M.; Fernandes, A. R.; Silva, J.; Mahmudov, K. T.; Guedes da Silva, M. F. C.; Pombeiro, A. J. L. Water Soluble Heterometallic Potassium-Dioxidovanadium(V) complexes as Potential Antiproliferative Agents. *J. Inorg. Biochem.* **2016**, *155*, 17. DOI: 10.1016/j.jinorgbio.2015.11.010.

[28] Vinhas, R.; Fernandes, A. R.; Baptista, P. V. Gold Nanoparticles for BCR-ABL1 Gene Silencing: Improving Tyrosine Kinase Inhibitor Efficacy in Chronic Myeloid Leukemia. *Mol. Ther. Nucleic Acids.* **2017**, *7*, 408. DOI: 10.1016/j.omtn.2017.05.003.

[29] Fernandes, A. R.; Jesus, J.; Martins, P.; Figueiredo, S.; Rosa, D.; Martins, L. M. R. D. R. S.; Corvo, M. L.; Carvalheiro, M. C.; Costa, P. M.; Baptista, P. V. Multifunctional Gold-Nanoparticles: A Nanovectorization Tool for the Targeted Delivery of Novel Chemotherapeutic Agents. *J. Contro.l Release.* **2017**, *245*, 52. DOI: 10.1016/j.jconrel.2016.11.021.

[30] Strobber, W. Trypan Blue Exclusion Test of Cell Viability. In *Current Protocols in Immunology*; John Wiley & Sons, Inc.: Hoboken, NJ, USA, **2001**; Vol. Appendix 3, pp Appendix 3B.

[31] Araújo, D.; Concórdio-Reis, P.; Marques, A. C.; Sevrin, C.; Grandfils, C.; Alves, V. D.; Fortunato, E.; Reis, M. A. M.; Freitas, F. Demonstration of the Ability of the Bacterial Polysaccharide FucoPol to Flocculate Kaolin Suspensions. *Environ. Technol.* **2019**, 1–9. DOI: 10.1080/09593330.2018.1497710.

[32] Farinha, I.; Duarte, P.; Pimentel, A.; Plotnikova, E.; Chagas, B.; Mafra, L.; Grandfils, C.; Freitas, F.; Fortunato, E.; Reis, M. A. M. Chitin-Glucan Complex Production by *Komagataella pastoris*: Downstream Optimization and Product Characterization. *Carbohydr Pol.* **2015**, *130*, 455–464. DOI: 10.1016/j.carbpol.2015.05.034.

[33] Synytsya, A.; Copikova, J.; Matejka, P.; Machovic, V. Fourier Transform Raman and Infrared Spectroscopy of Pectins. *Carbohydr. Pol.* **2003**, *54*, 97–106. DOI: 10.1016/S0144-8617(03)00158-9.

[34] Pramanik, A.; Maiti, S.; Mahanty, S. Metal Hydroxides as a Conversion Electrode for Lithium-Ion Batteries: A Case Study with a $Cu(OH)_2$ Nanoflower Array. *J. Mater. Chem. A.* **2014**, *2*, 18515. DOI: 10.1039/C4TA03379E.

[35] Abd El-Mohdy, H. L. Radiation Synthesis of Nanosilver/Poly Vinyl Alcohol/Cellulose Acetate/Gelatin Hydrogels for Wound Dressing. *J. Pol. Res.* **2013**, *20*, 177. DOI: 10.1007/s10965-013-0177-6.

[36] Ruiz, L. M.; Jensen, E. L.; Rossel, Y.; Puas, G. I.; Gonzalez-Ibanez, A. M.; Bustos, R. I.; Ferrick, D. A.; Elorza, A. A. Non-Cytotoxic Copper Overload Boosts Mitochondrial Energy Metabolism to Modulate Cell Proliferation and Differentiation in the Human Erythroleukemic Cell Line K562. *Mitochondrion.* **2016**, *29*, 18. DOI: 10.1016/j.mito.2016.04.005.

[37] Vinhas, R.; Lourenço, L.; Santos, S.; Ribeiro, P.; Silva, M.; de Sousa, A. B.; Baptista, P. V.; Fernandes, A. R. A Double Philadelphia Chromosome-Positive Chronic Myeloid Leukemia Patient, Co-expressing P210BCR-ABL1 and P195BCR-ABL1 Isoforms. *Haematologica.* **2018**, *103*, e549–e552. DOI: 10.3324/haematol.2018.192534.